Eigenvalue Computation for Application of the Finite Hankel Transform in Coaxial Regions

Z.A. Delecki

Department of Electrical Engineering
University of Ottawa
Ottawa, Canada K1N 6N5

Abstract

The evaluation of eigenvalues for transcendental equations in the cylindrical coordinate system is considered. A new code has been developed for this purpose. This is a fast algorithm for finding contours of a real function of two variables. This algorithm searches for the interval in which the function passes through the desired reference value and subsequently automatically starts to trace the contour within a circular annulus region of interest. When the reference value is zero and the function represents the limiting form of the Finite Hankel Transform kernel, the solution of the transcendental equation for eigenvalues is obtained. For accurate values of proper numbers, another code provides them within the desired uncertainty. Numerical results are presented and compared with available data. The computed eigenvalues may be used to obtain solutions of boundary value problems for circularly-symmetric electromagnetic waveguides, cables, cavities or scatterers.

1. Introduction

The solution of boundary value problems in multiply connected regions requires the specification of boundary conditions on every surface. The simplest structures belonging to this class are coaxial waveguides or cavities. The use of the finite integral transforms with respect to space variables considerably simplifies the solution of the boundary value problems. (The theoretical background is given in [1].) Appendix A provides more details regarding properties of the Finite Hankel Transform. For problems described in cylindrical coordinate systems, the Finite Hankel Transform offers a comparatively simple tool for solving the mixed boundary value problem for the Helmholtz equation. In spite of this, it has not obtained a wide enough dissemination. There is no known application of this method to the solution of practical problems in electromagnetics. The method has been used outside electromagnetics [2], but the applications have been limited. The reason for this is a lack of tabulation of roots of transcendental equations associated with the appropriate kernel of the Finite Hankel Transform [3]. However, as is shown in [4], there is the lack of the complete tabulation of zeros of two basic transcendental equations for the coaxial line. The existence, ordering and computation of these roots are necessary for applications of dyadic Green's functions for the coaxial line. Therefore, it is needed to verify and extend the existing tables. The largest existing tables of Bessel functions [5] are not sufficient to provide all needed values for computation of kernels of Finite Hankel Transform for problems of interest; they do not contain Neumann functions and are extremely laborious to use. Another problem to overcome is to compute Bessel and Neumann functions with the desired accuracy for the required order and argument.

The modern applications require numerical results. A condition for this is to provide the tables of roots χ_{mn} for the desired value of parameter $\ell = a/b$. Parameter ℓ is a limiting value of the normalized radius $\rho = r/b$ of a circular annulus when $r \to a$. The normalization of the radius implies that $\ell \leq \rho \leq 1$. For this domain, there are nine possible combinations of boundary conditions which include: Dirichlet $\Psi = 0$, Neumann

$\partial\Psi/\partial r = 0$ and Cauchy $\partial\Psi/\partial r + \alpha\Psi = 0$ [3]. In effect, nine transcendental equations result. Two symmetric cases, Dirchlet-Dirichlet (D-D) and Neumann-Neumann (N-N), are fundamental both from practical and theoretical points of view in electromagnetics. The first gives rise to TM_{mn} modes while the second gives rise to TE_{mn}. Because of the advent of optical fibre transmission technology, the higher order modes are again of interest to researchers [6].

2. Formulation

For annular domains with symmetric Dirichlet boundary conditions (D-D), the following transcendental equation is obtained:

$$J_m(\chi_{mn})Y_m(\chi_{mn}\ell) - Y_m(\chi_{mn})J_m(\chi_{mn}\ell) = 0 \ . \tag{1}$$

When symmetric Neumann boundary conditions (N-N) are applied, the transcendental equation is

$$J'_m(\chi_{m\,n})Y'_m(\chi_{m\,n}\ell) - J'_m(\chi_{m\,n}\ell)Y'_m(\chi_{m\,n}) = 0 \ . \tag{2}$$

In both equations, χ_{mn} is the eigenvalue and $\ell = a/b$ is the characteristic dimension of the coaxial structure. Indexes m and n denote order of Bessel or Neumann functions and number of root (or alternatively zero), respectively. These equations have the following properties [7] as $\ell \to 0$:

- the eigenvalues of (1) approach the corresponding root of

$$J_m(\chi) = 0 \ ; \tag{3}$$

- and the eigenvalues of (2) approach the corresponding root of

$$J'_m(\chi) = 0 \ . \tag{4}$$

The most extensive table of roots of (1) and (2) has been published [8]. In fact, (1) is tabulated up to the order $m = 3$ of Bessel function and up to 5-th root for limited

number of parameter ℓ. This is not sufficient for rigorous application of the FHT. For this reason, it is required that for any value of ℓ the eigenvalues be available, thus the points of characteristic equation lying in $\chi - \ell$ plane be linked so as to create $\ell(\chi)$ curves of zero contours.

3. The Algorithms

The nonlinear equations defined by (1) and (2) are also limiting forms of a kernel of the Finite Hankel Transform which is written in simplified form as

$$f_m(\chi, \ell) = 0 \tag{5}$$

with constrained arguments $0 < \chi \leq \chi_{max} < \infty$ and $0 \leq \ell < 1$. The detailed description of function (5) is given in Appendix A.

Two mutually-related codes were developed to accomplish this purpose: the first: for zero-contour determination $\ell(\chi)$ of equation (5); the second: for high accuracy eigenvalue χ_{mn} determination at constant value of ℓ.

The first one deals with 3-dimensional problems and allows us to determine properties of the characteristic dimension-eigenvalue domain $\ell - \chi$ and to obtain information about behavior of the function (and approximate location of all eigenvalues). This code uses a searching procedure (concept is described in [10], however, the details of the solution are different). Once bounds are imposed on both variables at boundaries of the region, in the parameter statement, the search procedure begins by examining values of function (5) on the perimeter of the $\chi - \ell$ plane. Each point on the perimeter is controlled by a component of a logical vector of which values are set to "true" at the beginning of the search process. For the search process along the boundary $\ell = 0$, the equations (3) and (4) are used. When brackets of the first eigenvalue are detected, the automatic search process is carried out.

The search procedure combines the Horn clause and state-space problem solving meth-

ods [9]. A logical grid function of two variables $G_{p,q}$ describes each grid. This function is defined as

$$G_{p,q} = C_p \& S_q \ . \tag{6}$$

The first argument C_p is generated by four logical node values n_s for $s = 1, 2, 3, 4$ defined as

$$n_s = \begin{cases} 0, & \text{if } f_m(\chi, \ell) < 0 \\ 1, & \text{if } f_m(\chi, \ell) \geq 0. \end{cases} \tag{7}$$

In order to determine C_p, the values of function f_m are examined at four vertices of the current grid. In effect, vector C_p may have sixteen distinct components, each of them associated with a combination of n_1, n_2, n_3, n_4 at vertices of a grid.

The second vector S_q has four components, each component is associated with each side of the grid. Components corresponding to the intersection of a grid side and the contour path assume logical value 1. The relation between components S_q^{t-1} of the last grid and components S_q^t of the present grid describes direction of the search process. The present value of the grid function $G_{p,q}^t$ represents the goal state while its past value $G_{p,q}^{t-1}$ represents the initial state. The goal state is determined from the initial state and actual values of C_p and S_q of a grid. The goal state of the present grid is identical to the initial state of the next grid. Only two states are permitted for every grid so as there is no ambiguity in determination of a goal state. The goal state determines the next grid to be examined, corresponding to values of the nodal variables i, j, and values of the contour coordinates χ_k and ℓ_k. These values are determined by an interpolation procedure using values of function $f_m(\chi, \ell)$ at points of the grid associated with its side corresponding to the new value of argument S_q. Function $G_{p,q}$ describes the search strategy in a systematic way. A demonstration of the grid function $G_{p,q}$ is shown in Fig. 1.

In this method, no rotation of a grid is required in contrast to code described in [10]. When the zero-contour is determined and its end point lies on the perimeter, a component of the logical vector controlling each perimeter point is set to false. The search procedure is then resumed on the perimeter from the following point from which the last eigenvalue

contour started. The detailed description of all aspects of the program will be presented by the author in a future article. The accuracy of the method is affected by the grid size.

The second code utilizes a similar technique of search, however, search strategy is carried out on components of a vector

$$f_m(\chi, \ell) = f_m(\chi) \qquad \text{for} \qquad \ell = const \tag{8}$$

where $\chi_{min} < \chi < \chi_{max}$. When the eigenvalue is bracketed, the iterative process starts. It uses a subroutine based on the modified Van Wijingaarden-Dekker-Brent Method [11]. This method combines root bracketing, bisection, and inverse quadratic interpolation. The program is capable of finding eigenvalues with the uncertainty of 10^{-8} at the expense of increase of computation time. The convergence of the code has been proven by numerical experiment, although, for large eigenvalues presented in Tab. 1.1 and Tab. 1.2, the number of iterations exceeds 200.

4. Computation

Computations ascertained by these two codes were performed on the Amdahl 5860, main University of Ottawa computer with the VM/CMS 4.2 operating system. Subroutines were written in VS/FORTRAN (FORTRAN-77) in double precision. The plotting software is in single precision so as to match the DISSPLA library. The evaluation of Bessel and Neumann functions was performed using the IMSL double precision library adapted from the NATS FUNPACK library [12]. The basic limitation is the machine precision which for double precision is 15 hexadecimal digits within the range $(10^{-78}, 10^{75})$.

The process of determination of the eigenvalue bracket of a transcendental equation is sometimes very difficult due to the lack of an algorithm which includes the sign change caused by a pole of the equation. However, this problem was not found to be very severe for equations (1) and (2).

5. Conclusions

For the illustration of the first code, equation (1) was chosen with index $m = 1$, i.e. the first non-rotationally symmetric TM_{mn} mode. In Fig.2 are depicted the transcendental function (1) and its zero contours projected onto $\chi - \ell$-plane. In Fig.3, the zero-contours in 2-D representation may be used directly in "approximate" engineering application. The accuracy of the first code suffers from the choice of the mesh size. Nevertheless, it provides quite good engineering presentation of eigenvalues.

In contrast with the first code, the second code provides high accuracy eigenvalues. Tables 1.1 and 1.2 show numerical values of eigenvalues of equation (1) with index $m = 1$. The uncertainty of each eigenvalue is ± 0.0001. These tables improve accuracy (over the first code and published data) of eigenvalues up to $n = 5$ and extend them up to $n = 100$ for $\ell = 0.100, 0.250, 0.333$, $n = 79$ for $\ell = 0.500$, $n = 51$ for $\ell = 0.667$ and $n = 26$ for $\ell = 0.833$. The code has been tested up to order $m = 54$ of transcendental functions and number of eigenvalue $n = 100$. These data pave the way for application of the Finite Hankel Transform to the solution of boundary value problems in various circular symmetry electromagnetic objects. The described code and its technical manual are available from the author.

5. Acknowledgments

The author wishes to acknowledge the doctoral scholarship provided by Natural Sciences and Engineering Research Council of Canada which made this research possible.

The author would also like to express his appreciation to Dr. Michał Mrozowski of Telecommunication Institute, Technical University of Gdańsk, Poland for providing the code described in [10], so the comparison of two solutions was possible.

6. References

[1] G.N. Watson, "A Treatise on the Theory of Bessel Functions", Cambridge University Press, 1966, pp. 576-582.

[2] H.S. Carslaw and J.C. Jaeger, "Conduction of Heat in Solids", Oxford at Clarendon Press, 1959, pp. 188-229.

[3] G. Cinelli, "An Extension of the Finite Hankel Transform and Applications", International Journal of Engineering Science, V. 3, No.5, 1965, pp. 539-559.

[4] Chen-To Tai, "Dyadic Green's Function for a Coaxial Line", IEEE Trans. on Antennas & Propag., V. AP-31, No.2, 1983, pp. 355-358.

[5] The Staff of the Comput. Lab. of Harvard University, "The Annals of the Computation Laboratory of Harvard University", Cambridge, Massachusetts, Harvard University, 1949.

[6] H.M. Barlow, "Optical Fibre Transmission in the TE_{mn} Mode", Journal of Physics, D: Applied Physics, V. 13, 1980, pp. 369-75.

[7] M. Kline, "Some Bessel Equations and Their Application to Guide and Cavity Theory", Journal of Mathematical Physics, V. 28, 1950, pp. 37-48.

[8] H.B. Dwight, "Table of Roots for Natural Frequencies in Coaxial Type Cavities", Journal of Mathematical and Applied Physics, v. 27, 1948, pp.90-97.

[9] R. Kowalski, "Logic for Problem Solving", North-Holland, New York, 1985, pp. 99-104 and 133-146.

[10] M. Mrozowski, "An Efficient Algorithm for Finding Zeros of a Real Function of Two Variables", IEEE Trans. on Microwave Theory and Tech., V. 36, No. 3, March 1988, pp. 601-604.

[11] W.H. Press, B.P. Flannery, S.A. Teukolsky, W.T. Vettering, "Numerical Recipes", Cambridge University Press, Cambridge, 1986, p. 269.

[12] National Activity to Test Software (NATS) FUNPACK, Argonne National Laboratory, Argonne Code Center, Argonne, Illinois 60439, 1976.

APPENDIX A

Finite Hankel Transform

Any twice differentiable function $f(\rho)$ that satisfies the boundary condition of a boundary value problem, say over $(\ell, 1)$, may be expanded into a uniformly convergent series of the normal orthogonal set of eigenfunctions pertaining to that boundary-value problem.

For a coaxial domain with the normalized radius $\rho = r/b$, where $\ell \leq \rho \leq 1$, the Finite Hankel Transform is defined as

$$\mathcal{F}(\chi, \ell) = \int_{\ell}^{1} f(\rho)\rho\mathcal{K}_m(\chi\rho)d\rho \ , \tag{A.1}$$

where $\mathcal{K}_m(\chi\rho)$ is the appropriate kernel pertaining to boundary conditions of the domain under consideration.

For TM_{mn} waves in coaxial waveguide or cavity with variation of the normalized radius $\ell \leq \rho \leq 1$, the kernel of the transformation becomes

$$\begin{aligned} \mathcal{K}_m(\chi\rho) &= \mathcal{K}_{DDm}(\chi\rho) \\ &= J_m(\chi\rho)Y_m(\chi\ell) - Y_m(\chi\rho)J_m(\chi\ell) \end{aligned} \tag{A.2}$$

by the well-known theory of Fourier-Bessel series [1]. For this case, the inverse formula is

$$f_{DD}(\rho) = \frac{\pi^2}{2}\sum_{k=1}^{K} \frac{\chi_k^2 J_m^2(\chi_k)}{J_m^2(\chi_k\ell) - J_m^2(\chi_k)}\mathcal{F}(\chi_k\ell)\mathcal{K}_{DDm}(\chi_k\rho) \ , \tag{A.3}$$

where K denotes the summation limit, in general K $\rightarrow \infty$, while χ_k are positive roots (zeros) of the transcendental equation:

$$\begin{aligned} f_m(\chi\ell) = \lim_{\rho\to 1}\mathcal{K}_{DDm}(\chi\rho) &= J_m(\chi)Y_m(\chi\ell) - Y_m(\chi)J_m(\chi\ell) \\ &= 0 \ . \end{aligned} \tag{A.4}$$

For TE waves, the kernel of transformation

$$\begin{aligned}\mathcal{K}_m(\chi\rho) &= \mathcal{K}_{NNm}(\chi\rho) \\ &= J_m(\chi\rho)Y'_m(\chi\ell) - Y_m(\chi\rho)J'_m(\chi\ell)\ . \end{aligned} \tag{A.5}$$

The inverse formula for this case is given as

$$f_{NN}(\rho) = \\ = \frac{\pi^2}{2}\sum_{k=1}^{K} \frac{\chi_k^2[J'_m(\chi_k)]^2}{[J'_m(\chi_k\ell)]^2\left[1-\left(\frac{m}{\chi_k}\right)^2\right] - \left[J'_m(\chi_k)\right]^2\left[1-\left(\frac{m}{\chi_k\ell}\right)^2\right]}\mathcal{F}(\chi_k\ell)\mathcal{K}_{NNm}(\chi_k\rho)\ , \tag{A.6}$$

where χ_k are roots of the transcendental equation:

$$\begin{aligned} f_m(\chi\ell) = \lim_{\rho\to 1}\frac{\partial\mathcal{K}_{NNm}(\chi\rho)}{\partial\rho} &= \chi\left[J'_m(\chi)Y'_m(\chi\ell) - Y'_m(\chi)J'_m(\chi\ell)\right] \\ &= 0\ . \end{aligned} \tag{A.7}$$

Discrete roots of equations (A.4) and (A.7) χ_k are found by the numerical procedure described in the article. Index k in (A.3) and (A.6) is identical with index n in (1) and (2), if computed eigenvalues χ_k are known with the uncertainty equal to zero. However, the uncertainty existence in the determination of eigenvalues implies that $\chi_k \neq \chi_n$, therefore the use of k is reserved for eigenvalues computed with errors. Expansions (A.3) and (A.6) represent one of two possible expansions of functions $f_{DD}(\rho)$ and $f_{NN}(\rho)$ in each region, respectively [3].

p	n_1	n_2	n_3	n_4
1	0	0	0	0
2	0	0	0	1
3	0	0	1	0
4	0	0	1	1
5	0	1	0	0
6	0	1	0	1
7	0	1	1	0
8	0	1	1	1
9	1	0	0	0
10	1	0	0	1
11	1	0	1	0
12	1	0	1	1
13	1	1	0	0
14	1	1	0	1
15	1	1	1	0
16	1	1	1	1

$G_{p,q}^{t-1} = C_7 \& S_3 = 1$ initial state

$G_{7,3}^{t-1} \rightarrow G_{3,2}^{t} = G_{3,4}^{t} = 1$ goal state

$G_{3,4}^{t} \rightarrow i = i + 1,\ k = k$

For the adjacent grid sides:
$S_1^t = S_3^t$
$S_2^t = S_4^t$

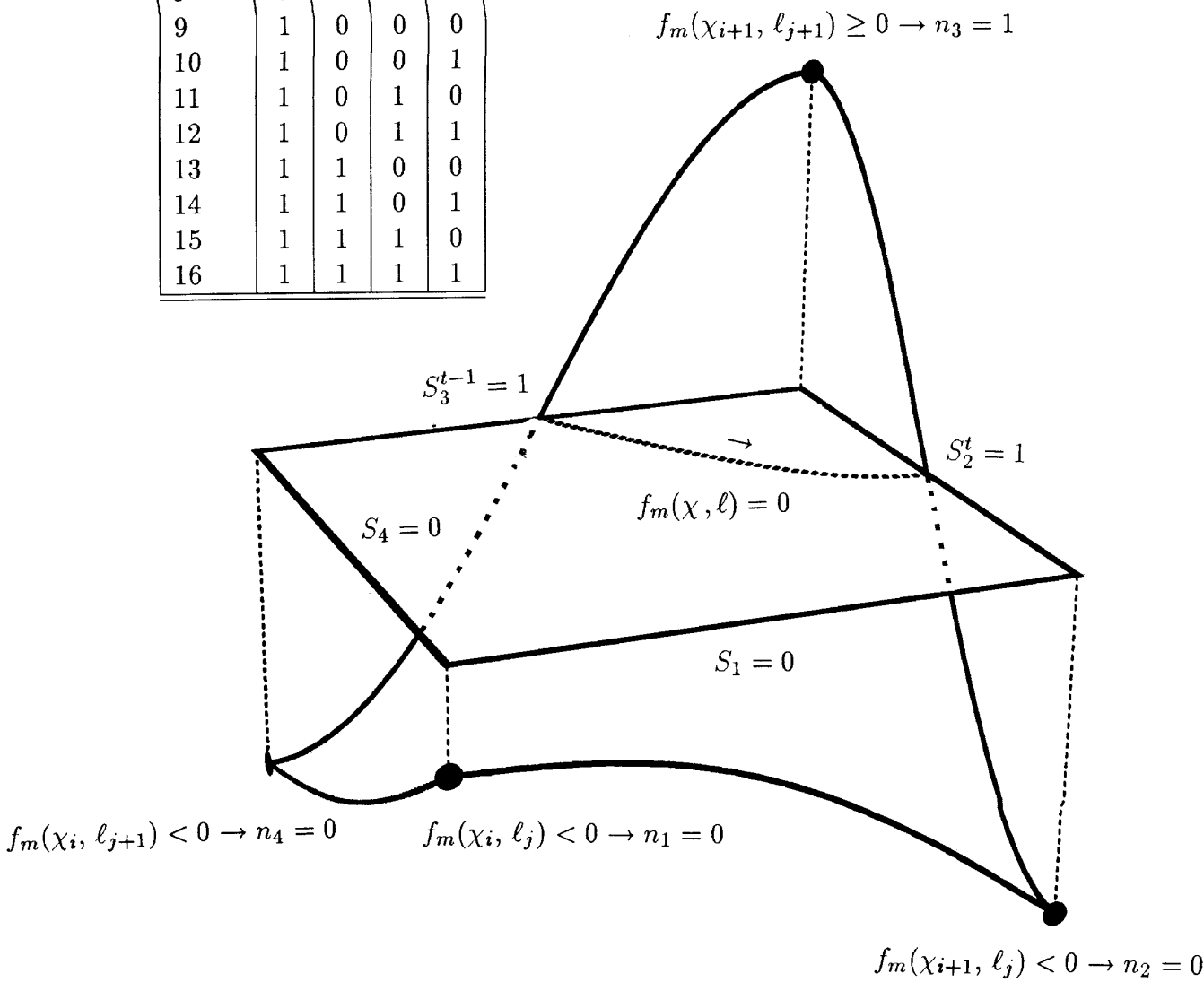

Fig. 1

Demonstration of the grid function $G_{p,q}$ for a grid along the search path. The table presents generation of the index p by nodal values n_1, n_2, n_3, n_4.

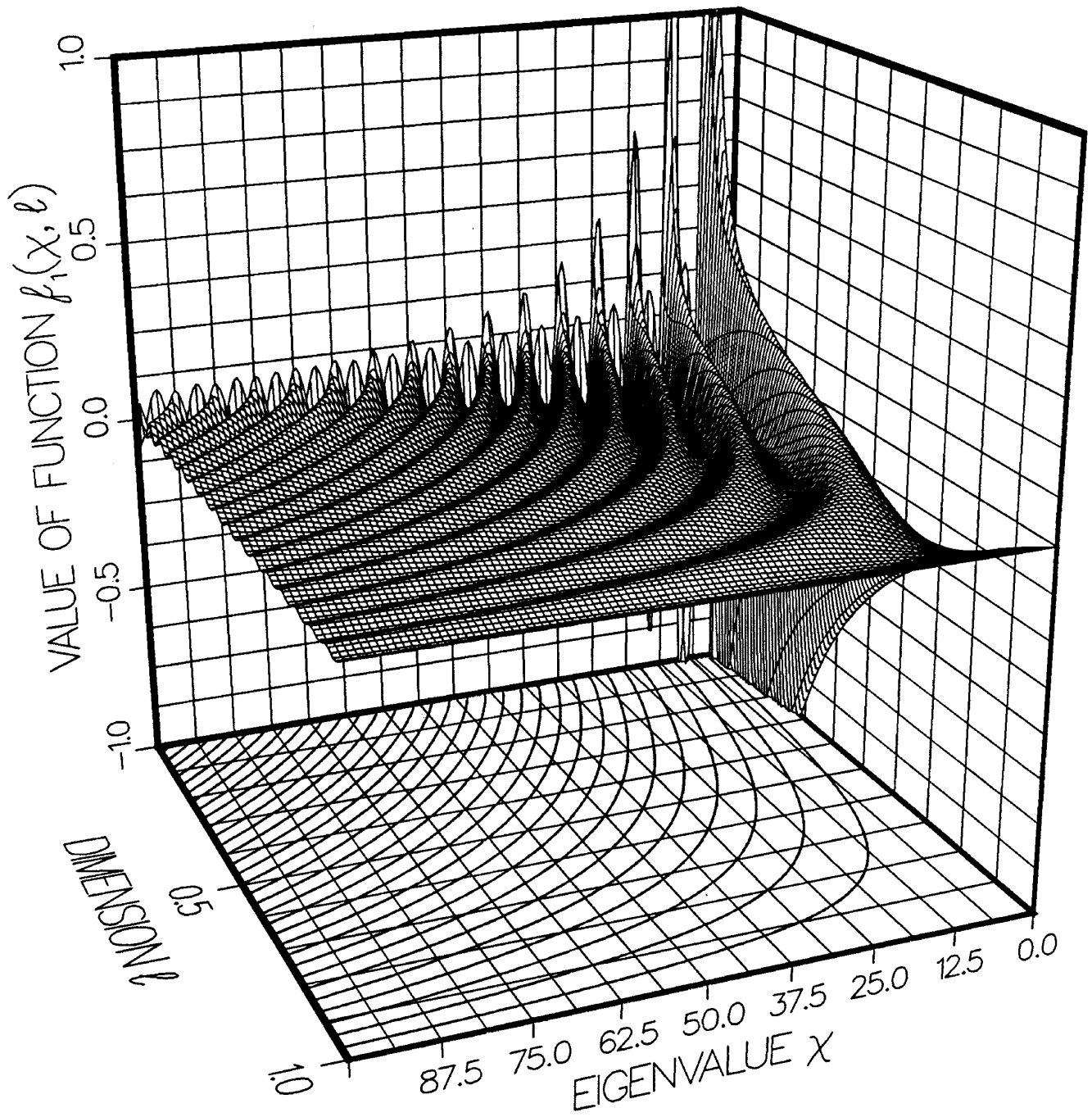

Fig. 2

Transcendental function $f_1(\chi, \ell)$ and its zero contour projected onto $\chi - \ell$ plane.

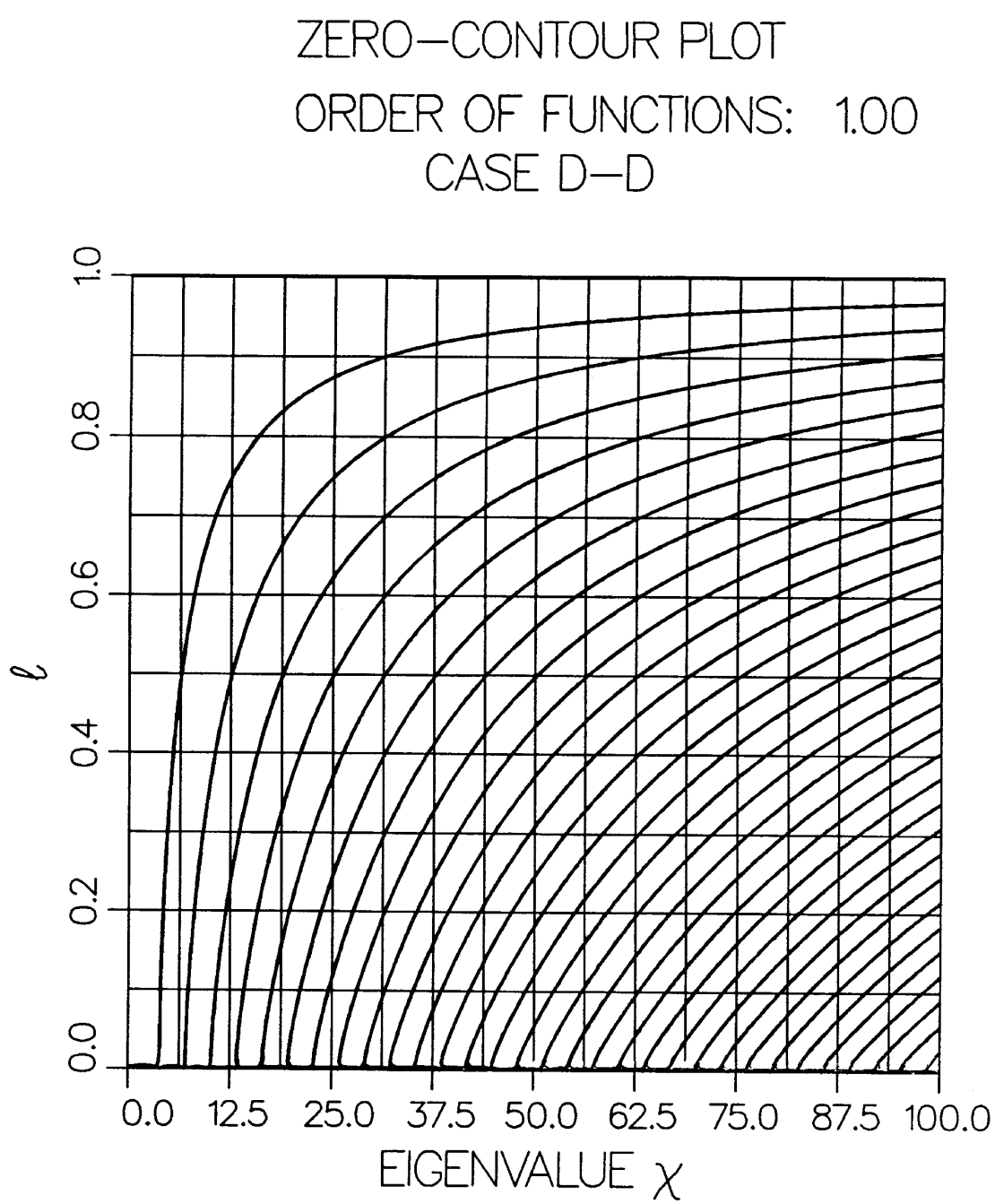

Fig. 3

2-D representation of the solution of the transcendental equation $f_1(\chi, \ell) = 0$.

Roots χ_{1n} of the transcendental equation $J_1(\chi_{1n})Y_1(\chi_{1n}\ell) - J_1(\chi_{1n}\ell)Y_1(\chi_{1n}) = 0$						
n	$\ell = 0.100$	$\ell = 0.250$	$\ell = 0.333$	$\ell = 0.500$	$\ell = 0.667$	$\ell = 0.833$
1	3.9502	4.4502	4.9252	6.4003	9.5005	18.8509
2	7.3254	8.5254	9.5255	12.6006	18.8759	37.6269
3	10.7505	12.7006	14.2257	18.9009	28.3264	56.4528
4	14.1757	16.8258	18.8759	25.1512	37.7269	75.2287
5	17.6509	21.0260	23.6012	31.4516	47.2023	94.0797
6	21.1010	25.1763	28.2764	37.7019	56.6028	112.8556
7	24.6012	29.3764	33.0266	44.0022	66.0533	131.7066
8	28.0514	33.5517	37.7019	50.2775	75.4788	150.4825
9	31.5516	37.7519	42.4271	56.5778	84.9292	169.3334
10	35.0017	41.9021	47.1023	62.8281	94.3297	188.1094
11	38.5019	46.1273	51.8526	69.1284	103.8052	206.9353
12	41.9521	50.2775	56.5278	75.4037	113.2056	225.7363
13	45.4773	54.5027	61.2531	81.7041	122.6561	244.5622
14	48.9274	58.6529	65.9533	87.9544	132.0816	263.3630
15	52.4526	62.8781	70.6785	94.2797	141.5320	282.1887
16	55.9028	67.0283	75.3537	100.5300	150.9325	300.9900
17	59.4279	71.2535	80.1040	106.8303	160.4080	319.8157
18	62.8781	75.4037	84.7792	113.0806	169.8085	338.5918
19	66.4033	79.6290	89.5045	119.4059	179.2589	357.4424
20	69.8535	83.7792	94.2047	125.6562	188.6844	376.2187
21	73.3786	88.0044	98.9299	131.9566	198.1349	395.0696
22	76.8288	92.1546	103.6302	138.2319	207.5353	413.8455
23	80.3540	96.3798	108.3554	144.5322	217.0108	432.6965
24	83.8042	100.5300	113.0306	150.7825	226.4113	451.4724
25	87.3293	104.7552	117.7809	157.1078	235.8618	470.3232
26	90.7795	108.9054	122.4561	163.3581	245.2872	489.0994
27	94.3047	113.1306	127.1813	169.6584	254.7377	
28	97.7549	117.2808	131.8816	175.9088	264.1379	
29	101.2800	121.5061	136.6068	182.2341	273.6133	
30	104.7552	125.6562	141.3070	188.4844	283.0139	
31	108.2554	129.8815	146.0323	194.7847	292.4641	
32	111.7306	134.0317	150.7075	201.0600	301.8899	
33	115.2307	138.2569	155.4577	207.3603	311.3401	
34	118.7059	142.4071	160.1330	213.6106	320.7410	
35	122.2061	146.6323	164.8582	219.9360	330.2161	
36	125.6813	150.7825	169.5584	226.1863	339.6167	
37	129.2064	155.0077	174.2837	232.4866	349.0920	
38	132.6566	159.1829	178.9839	238.7619	358.4927	
39	136.1818	163.3831	183.7092	245.0622	367.9431	
40	139.6320	167.5583	188.3844	251.3125	377.3687	
41	143.1571	171.7586	193.1346	257.6375	386.8191	
42	146.6323	175.9338	197.8099	263.8879	396.2197	
43	150.1325	180.1340	202.5601	270.1880	405.6951	
44	153.6077	184.3092	207.2353	276.4387	415.0955	
45	157.1078	188.5094	211.9606	282.7637	424.5461	
46	160.5830	192.6846	216.6608	289.0144	433.9714	
47	164.1082	196.8848	221.3860	295.3145	443.4219	
48	167.5583	201.0600	226.0863	301.5898	452.8225	
49	171.0835	205.2602	230.8115	307.8899	462.2979	
50	174.5337	209.4354	235.4867	314.1406	471.6985	

Tab. 1.1

Roots of the transcendental equation $f_1(\chi, \ell) = 0$ with the uncertainty ± 0.0001 for the D-D case.

Roots χ_{1n} of the transcendental equation $J_1(\chi_{1n})Y_1(\chi_{1n}\ell) - J_1(\chi_{1n}\ell)Y_1(\chi_{1n}) = 0$						
n	$\ell = 0.100$	$\ell = 0.250$	$\ell = 0.333$	$\ell = 0.500$	$\ell = 0.667$	$\ell = 0.833$
51	178.0589	213.6357	240.2370	320.4656	481.1489	
52	181.5340	217.8109	244.9122	326.7161	490.5742	
53	185.0342	222.0361	249.6374	333.0164		
54	188.5094	226.1863	254.3377	339.2917		
55	192.0096	230.4115	259.0625	345.5918		
56	195.4847	234.5617	263.7629	351.8425		
57	199.0099	238.7869	268.4880	358.1675		
58	202.4601	242.9371	273.1636	364.4180		
59	205.9853	247.1623	277.9136	370.7183		
60	209.4354	251.3125	282.5889	376.9687		
61	212.9606	255.5377	287.3389	383.2939		
62	216.4358	259.6877	292.0144	389.5442		
63	219.9360	263.9128	296.7395	395.8447		
64	223.4111	268.0632	301.4399	402.1199		
65	226.9113	272.2883	306.1648	408.4202		
66	230.3865	276.4636	310.8655	414.6707		
67	233.9117	280.6636	315.5903	420.9958		
68	237.3618	284.8391	320.2659	427.2461		
69	240.8870	289.0391	325.0159	433.5464		
70	244.3372	293.2146	329.6914	439.8218		
71	247.8624	297.4146	334.4163	446.1221		
72	251.3375	301.5898	339.1167	452.3723		
73	254.8377	305.7898	343.8418	458.6978		
74	258.3127	309.9653	348.5422	464.9480		
75	261.8376	314.1653	353.2673	471.2483		
76	265.2881	318.3408	357.9426	477.4988		
77	268.8130	322.5657	362.6926	483.8240		
78	272.2634	326.7161	367.3682	490.0742		
79	275.7883	330.9412	372.1184	496.3745		
80	279.2639	335.0916	376.7937			
81	282.7637	339.3167	381.5188			
82	286.2393	343.4670	386.2192			
83	289.7390	347.6919	390.9443			
84	293.2146	351.8425	395.6445			
85	296.7395	356.0674	400.3699			
86	300.1899	360.2178	405.0452			
87	303.7148	364.4429	409.7954			
88	307.1653	368.5933	414.4705			
89	310.6902	372.8184	419.1958			
90	314.1655	376.9937	423.8960			
91	317.6655	381.1938	428.6213			
92	321.1409	385.3691	433.3215			
93	324.6658	389.5693	438.0466			
94	328.1162	393.7446	442.7219			
95	331.6411	397.9448	447.4722			
96	335.0916	402.1199	452.1475			
97	338.6165	406.3201	456.8977			
98	342.0920	410.4954	461.5730			
99	345.5918	414.6956	466.2981			
100	349.0674	418.8708	470.9983			

Tab. 1.2

Roots of the transcendental equation $f_1(\chi, \ell) = 0$ with the uncertainty ± 0.0001 for the D-D case.